Inflammatory Bowel Disease: How Effective Is TNF-α Suppression?

Wing-Cheong Lo[1]*, Violeta Arsenescu[2], Razvan I. Arsenescu[3], Avner Friedman[4]

1 Department of Mathematics, City University of Hong Kong, Hong Kong, Hong Kong SAR, 2 Armedica LLC, Dublin, Ohio, United States of America, 3 Digestive Health Institute, Inflammatory Bowel Diseases Center of Excellence Morristown Medical Center, Morristown, New Jersey, United States of America, 4 Mathematical Biosciences Institute, Department of Mathematics, The Ohio State University, Columbus, Ohio, United States of America

* wingclo@cityu.edu.hk

Abstract

Crohn's Disease (CD) results from inappropriate response toward commensal flora. Earlier studies described CD as a Th1 mediated disease. Current models view both phenotypes as a continuum of various permutations between Th1, Th2 and Th17 pathways compounded by a range of Treg disfunctions. In the present paper, we develop a mathematical model, by a system of differential equations, which describe the dynamic relations among these T cells and their cytokines. The model identities four groups of CD patients according to up/down regulation of Th1 and Th2. The model simulations show that immunosuppression by TNF-α blockage benefits the group with $Th1^{High}/Th2^{Low}$ while, by contrast, the group with $Th1^{Low}/Th2^{High}$ will benefit from immune activation.

Introduction

Inflammatory Bowel Diseases (IBD), Crohn's Disease (CD) and Ulcerative Colitis (UC) result from an inappropriate immune response toward commensal flora [1]. Genome wide association studies (GWAS) indicated that the majority of IBD susceptibility loci belong to immunoregulatory networks [2, 3].

Patients with inflammatory bowel diseases have elevated levels of circulating and gut mucosal cytokines [1]. Downstream signaling from these inflammatory mediators, through Janus kinase (JAK) and signal transducers and activators of transcription (STAT) proteins, activate transcription factors T-bet, GATA3, Foxp3 and RORγt [3]. A complex network of regulatory feedback loops involving these cytokines and their targets, are responsible for the polarization of naïve T cells into specific T helper cells: Th1, Th2, Th17 and Treg [3, 4].

Earlier animal and human studies described CD as a Th1 mediated [5]. Current models view both phenotypes as a continuum of various permutations between the Th1, Th2, and Th17 pathways compounded by a range of Treg dysfunctions [4].

The development of current biological therapies in CD, mirrors our understanding of immune regulatory pathways. Unfortunately the clinical triage of CD patients, based on Montreal classification, cannot identify relevant immune targets in a given patient [6]. Thus our treatments are inherently a trial and error approach. Pretreatment knowledge of the relevant gut mucosal immune

dysfunction in a given patient would significantly improve the risk/benefit balance and open the way toward personalized medical care. We have previously developed a theoretical model that described the relationship between Th1, Th2 and Treg circuits in patients with CD [7]. Our current study expands this model to include the Th17 pathway which plays an important role in inhibiting Treg cell differentiation that associated with autoimmune disorders and inflammation [8, 9]. The levels of Th17 cell transcription factor and related cytokines have been collected in our clinical data to provide better predictions of disease outcome through our new model. Furthermore, based on patients' data, it allowed us to simulate the effect of TNF-α suppression in a cohort of patients with CD, and thus identify distinct groups which will benefit from TNF-α suppression and groups which may benefit from immune activation rather than immune suppression.

Materials and Methods

Mathematical model

A system of differential equations was developed based on the network that incorporates cytokines and transcriptions factors relevant to Th1, Th2, Th17 and regulatory T cells pathway as shown in Fig 1. The relative concentrations of either immune cells or inflammatory mediators were defined in g/cm^3 and were based on a theoretical density in a cm^3 of tissue. The variables (concentrations) included in the model are listed in Table 1.

Differential equations for cytokines. IFN-γ is produced by Th1 cells and activates M1 macrophages [10]. In order to derive an equation which expresses the dynamics of I_γ, we denote by dI_γ the change in I_γ over a small time interval dt, and compute the quotient dI_γ/dt (the derivative of I_γ with respect to t, if dt is infinitesimally small). If I_γ is produced by Th1 cells and the production rate coefficient for IFN-γ by Th1 cells is $v_{\gamma 1}$, then, at a given Th1 cell density T_1, we can write $dI_\gamma/dt = v_{\gamma 1}T_1$. Similarly, the production of this cytokine by activated macrophages would be described by the differential equation $dI_\gamma/dt = v_{\gamma M}M_1$. We finally have to account for the fact that IFN-γ tissue concentration decays at some known rate δ_γ. Therefore the final formula for the dynamics of I_γ is given by the differential equation:

$$\frac{dI_\gamma}{dt} = \underbrace{v_{\gamma M}M_1 + v_{\gamma 1}T_1}_{\text{Production}} - \underbrace{\delta_\gamma I_\gamma}_{\text{Decay}} . \tag{1}$$

Similar differential equations were established for IL-2, IL-4, IL-6, IL-21, TGF-β and TNF-α. IL-2 is secreted by Th1 cells [11, 12], so we have

$$\frac{dI_2}{dt} = \underbrace{v_{21}T_1}_{\text{Production}} - \underbrace{\delta_2 I_2}_{\text{Decay}} . \tag{2}$$

Th2 cells and M2 macrophages produce IL-4 during inflammation [4, 10, 13]; hence

$$\frac{dI_4}{dt} = \underbrace{v_{4M}M_2 + v_{42}T_2}_{\text{Production}} - \underbrace{\delta_4 I_4}_{\text{Decay}} . \tag{3}$$

IL-21 is produced by Th17 cells [14, 15], so that

$$\frac{dI_{21}}{dt} = \underbrace{v_{2117}T_{17}}_{\text{Production}} - \underbrace{\delta_{21} I_{21}}_{\text{Decay}} . \tag{4}$$
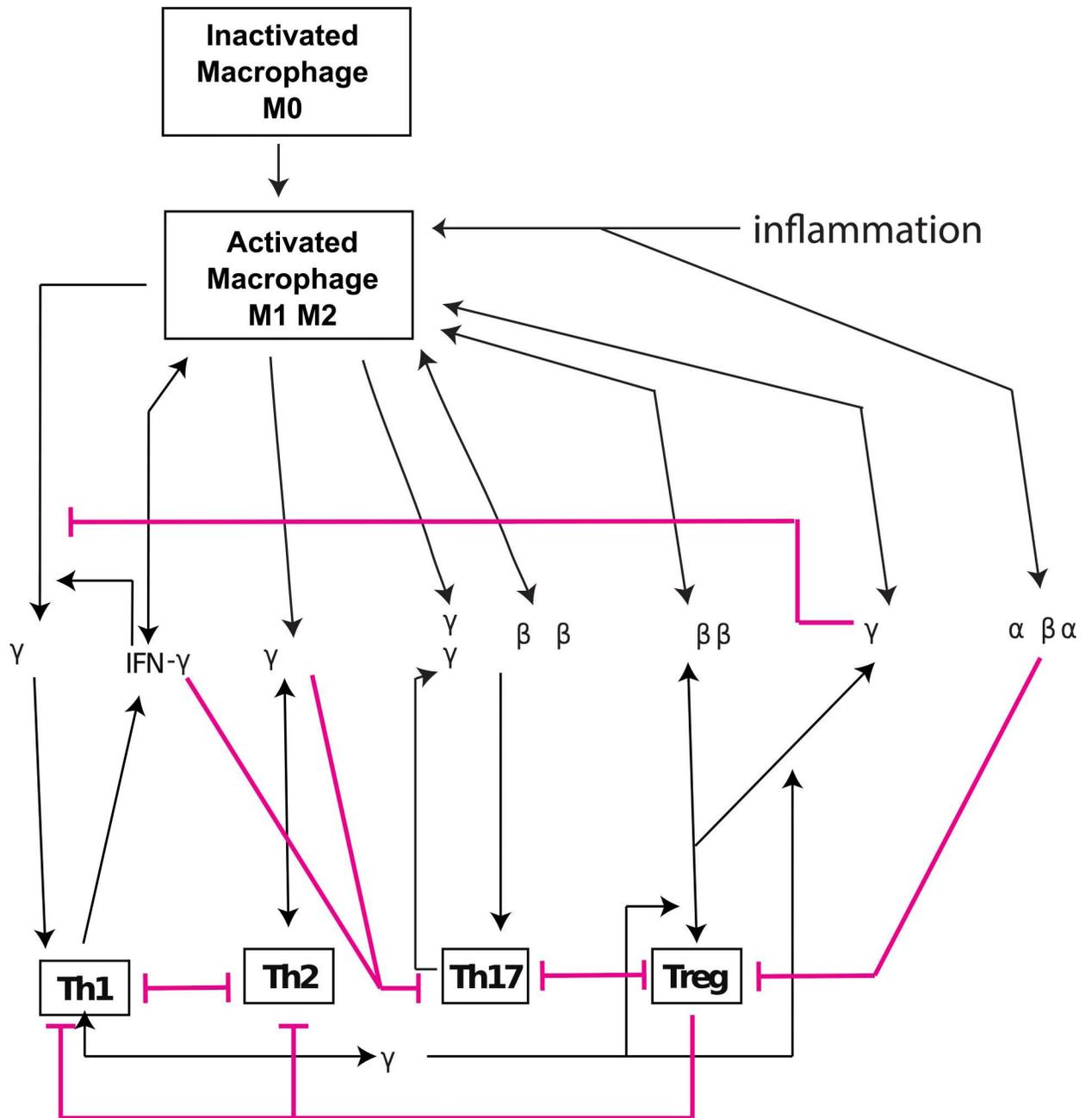
Fig 1. Schematic diagram of immune system with application to inflammatory bowel disease (IBD).

doi:10.1371/journal.pone.0165782.g001

IL-6 and TNF-α are produced by M1 [14, 15] and Th1 cells also produce TNF-α [16]; hence, the equations of I_6 and I_α are

$$\frac{dI_6}{dt} = \underbrace{v_{6M}M_1}_{\text{Production}} - \underbrace{\delta_6 I_6}_{\text{Decay}},$$

(5)

Table 1. List of the variables included in the model.

M_1: activated M1 macrophages	T_1: Th1 cells
M_2: activated M2 macrophages	T_2: Th2 cells
M: total macrophages ($M_1 + M_2$)	T_{17}: Th17 cells
I_α: TNF-α	I_β: TGF-β
I_γ: IFN-γ	I_2: IL-2
I_4: IL-4	I_6: IL-6
I_{10}: IL-10	I_{12}: IL-12
I_{21}: IL-21	

doi:10.1371/journal.pone.0165782.t001

$$\frac{dI_\alpha}{dt} = \underbrace{v_{\alpha M}M_1 + v_{\alpha 1}T_1}_{\text{Production}} - \underbrace{\delta_\alpha I_\alpha}_{\text{Decay}} . \tag{6}$$

TGF-β is mainly expressed from M2 macrophages and Treg cells [4, 10, 17]; hence we have

$$\frac{dI_\beta}{dt} = \underbrace{v_{\beta M}M_2 + v_{\beta r}T_r}_{\text{Production}} - \underbrace{\delta_\beta I_\beta}_{\text{Decay}} . \tag{7}$$

Cytokine IL-10 can be the product of both M2 macrophages and Treg cells [4, 10, 17], and IL-2 further increases IL-10 production by Treg cells [18]. IL-2 binds its cognate receptors and it is rapidly internalized. Allowing for the receptor recycling rate (n_{2r}) and maximum amount of IL-2 bound at any given time, we can write an equation that links this rate to the tissue concentration of IL-2 (I_2) and Treg (T_r): $n_{2r} (I_2/(\zeta_2 + I_2)) T_r$ where ζ_2 is a constant. Therefore the differential equation that incorporates IL-10 secretion from macrophages, Treg cells and IL-2 contribution can be written as:

$$\frac{dI_{10}}{dt} = \underbrace{v_{10M}M_2 + v_{10r}\left[1 + n_{2r}\left(\frac{I_\gamma}{\zeta_2 + I_2}\right)\right]T_r}_{\text{Production}} - \underbrace{\delta_{10}I_{10}}_{\text{Decay}} . \tag{8}$$

IL-12 is produced by M1 macrophages, and IL-10 can suppress its expression [19]. The IL-10 mediated suppression can be described using the expression ($1+ I_{10}/\zeta_{10}$) where ζ_{10} is a constant specific to IL-10 activation rate. Thus the differential equation for the net IL-12 production becomes:

$$\frac{dI_{12}}{dt} = \underbrace{v_{12M}\frac{M_1}{1 + I_{10}/\zeta_{10}}}_{\text{Production}} - \underbrace{\delta_{12}I_{12}}_{\text{Decay}} . \tag{9}$$

Differential equations for macrophages. The specific polarization of naïve T cells toward Th1, Th2, Th17 and Treg phenotypes is supported by cytokines produced by activated macrophages [4]. Activated macrophages fall into two major groups, M1 and M2. Increased tissue concentration of TNF-α in IBD patients can lead undifferentiated M0 macrophages to polarize to M1 macrophages, classically activated macrophages [20]. M1 macrophages can also be derived from M2 in the presence of high levels of IFN-γ, a proinflammatory cytokine [21]. In contrast, M2 (alternatively activated macrophages) are induced by anti-inflammatory cytokines such as IL-10 and TGF-β [21]. The following factors were considered when obtaining a

differential equation for M1 macrophage phenotype formation: concentration of tissue factors (f_1) that contribute to macrophage polarization; tissue concentrations of TNF-α (I_α), IFN-γ (I_γ) and TGF-β (I_β); cytokine specific rates of macrophage activation ($\sigma_{M\alpha}$, $\sigma_{M\beta}$, $\sigma_{M\gamma}$) and transition between M1 and M2 phenotypes ($\sigma_{M\beta}$, $\sigma_{M\gamma}$), and macrophage apoptosis (decay) rate (μ_M). The differential equation for M1 is given by

$$\frac{dM_1}{dt} = \underbrace{\left(f_1 + \sigma_{M\alpha}\frac{I_\alpha}{\zeta_\alpha + I_\alpha}\right)M_0}_{\text{M0}\rightarrow\text{M1 by TNF}-\alpha} - \underbrace{\sigma_{M\beta}\frac{I_\beta}{\zeta_\beta + I_\beta}M_1}_{\text{M1}\rightarrow\text{M2 by TGF}-\beta} + \underbrace{\sigma_{M\gamma}\frac{I_\gamma}{\zeta_\gamma + I_\gamma}M_2}_{\text{M2}\rightarrow\text{M1 by IFN}\gamma} - \underbrace{\mu_M M_1}_{\text{Decay}}. \tag{10}$$

Similarly, undifferentiated M0 macrophages polarize to M2 macrophages under the influence of IL-10 [22], while M1 convert to M2 macrophages by TGF-β [21], so that the complete formula for dM_2/dt, after including death rate (μ_M) is:

$$\frac{dM_2}{dt} = \underbrace{\left(f_2 + \sigma_{M10}\frac{I_{10}}{\zeta_{10} + I_{10}}\right)M_0}_{\text{M0}\rightarrow\text{M1 by IL10}} + \underbrace{\sigma_{M\beta}\frac{I_\beta}{\zeta_\beta + I_\beta}M_1}_{\text{M1}\rightarrow\text{M2 by TGF}-\beta} - \underbrace{\sigma_{M\gamma}\frac{I_\gamma}{\zeta_\gamma + I_\gamma}M_2}_{\text{M2}\rightarrow\text{M1 by IFN}\gamma} - \underbrace{\mu_M M_2}_{\text{Decay}}. \tag{11}$$

Differential equations for T cells. We finally turn to the dynamics of the T cells. The initiation of the inflammatory process involves macrophage activation. Macrophages produce several types of cytokines including IL-12, IFN-γ, IL-4, IL-6, TGF-β, IL-10 and TNF-α, and all these cytokines activate T cells upon binding to their specific receptors. The inflammatory network in IBD involves several auto-activation loops among the four types of T cells:

Th1 cells: As shown in Fig 1(A), the loop of Th1 auto-activation includes IL-12, IFN-γ, and macrophages. IL-12 induces Th1 activation while IFN-γ, produced by Th1 cells, activates macrophages to produce more IL-12 [10, 13].

Th2 cells: The loop of Th2 auto-activation includes IL-4 which leads to Th2 activation while Th2 cells further drive the expression of IL-4 [4, 10, 13]. This positive feedback loop is shown in Fig 1(B).

Th17 cells: Th17 auto-activation involves IL-6, IL-21 and TGF-β. Th17 cells induce production of IL-21 which, together with IL-6 and TGF-β, may further stimulate the activation of Th17 cells [8, 14, 15]. This is shown in Fig 1(C).

Treg cells: The loop of Treg auto-activation includes TGF-β, IL-10 and IL-2. As shown in Fig 1(D), TGF-β and IL-10 trigger Treg activation while Treg cells express TGF-β and IL-10, forming a positive feedback loop in Treg differentiation [4, 10, 17]. We assume that IL-2 is critical for the activation of Treg cells [23].

Aside from activation, the system is regulated by several inhibitory processes (red lines in Fig 1). Treg inhibits the activation of Th1 and Th2 cells [24] while the pairs, Th1-Th2 and Th17-Treg, are mutually antagonistic [9, 25]. IFN-γ produced by Th1 and IL-4 produced by Th2 inhibits Th17 activation [26].

Macrophages activation after encounter of microbial antigen induces Th1 development through direct contact and IL-12 production [10, 13]. Inhibition of IL-12 production by macrophages may explain the ability of IL-10 to suppress Th1 development [27]. Mathematically this is expressed by the following equation:

$$\frac{dT_1}{dt} = \sigma_{12}\frac{I_{12}}{\zeta_{12} + I_{12}}\frac{1}{1 + I_{10}/\zeta_{10}}M.$$

IL-2 secretion by Th1 cells can further enhance their activation [28]. On the other hand, negative regulatory signals are provided by Th2 and Treg cells [24, 25]. Finally the net rate of Th1 cell production needs to incorporate the activation-induced apoptosis. Hence our original differential equation becomes:

$$\frac{dT_1}{dt} = \underbrace{\left(\sigma_{12}\frac{I_{12}}{\zeta_{12}+I_{12}}\frac{1}{1+I_{10}/\zeta_{10}}M + \sigma_2\frac{I_2}{\zeta_2+I_2}T_1\right)}_{\text{Cytokine signaling}}\underbrace{\left(\frac{1}{1+T_2/\gamma_2}\right)\left(\frac{1}{1+T_r/\gamma_{r1}}\right)}_{\text{Inhibition by Th2, Treg}} - \underbrace{\mu_1 T_1}_{\text{Decay}}. \quad (12)$$

Similarly, for Th2 we accounted for IL-4 signaling, reciprocal Th2 inhibition by Th1 and Treg programs as well as activation-induced death of Th2 cells [4, 10, 13, 24]:

$$\frac{dT_2}{dt} = \underbrace{\left(\sigma_4\frac{I_4}{\zeta_4+I_4}M\right)}_{\text{Cytokine signaling}}\underbrace{\left(\frac{1}{1+T_1/\gamma_1}\right)\left(\frac{1}{1+T_r/\gamma_{r2}}\right)}_{\text{Inhibition by Th1, Treg}} - \underbrace{\mu_2 T_2}_{\text{Decay}}. \quad (13)$$

IL-6 in conjunction with TGF-β activates Th17 cells [8, 14, 15]. IL-21 is also a potent inducer of Th17 differentiation [8, 14, 15]; downregulation of IL-21 expression decreases Th17 cell infiltration in intestinal mucosa of IBD patients. Th17 activation is resisted by both IFN-γ and IL-4 [29]. Since Treg cells are also an inhibitor of Th17 activation [9], the final equation for T_{17} is:

$$\frac{dT_{17}}{dt} = \underbrace{\left[\left(\sigma_{21}\frac{I_{21}}{\zeta_{21}+I_{21}} + \sigma_6\frac{I_6}{\zeta_6+I_6}\right)\frac{I_\beta}{\zeta_\beta+I_\beta}\frac{M}{(1+I_\gamma/\zeta_\gamma)(1+I_4/\zeta_4)}\right]}_{\text{Cytokine signaling}}\underbrace{\left(\frac{1}{1+T_r/\gamma_{r17}}\right)}_{\text{Inhibition by Treg}} - \underbrace{\mu_{17} T_{17}}_{\text{Decay}}. \quad (14)$$

Treg cells number is regulated by a dynamic homeostatic process that balances high rates of cell division with apoptosis. These cells have high affinity for IL-2 which is a potent negative regulator of pro-apoptotic signals in Treg cells [23]. Interaction with innate immune cells like macrophages as well as cytokines like TGF-β and IL-10 promotes survival and immunosuppressive activity of this cell population. IBD patients have increased gut production of the proinflammatory cytokine TNF-α which was shown to increase Treg cell apoptosis, and TNF-α blockade can reverse this process, which is also observed in rheumatoid arthritis (RA) patients [30]. Proinflammatory cytokines that drive a Th17 response negatively regulate Treg cell development. Increased Th17 cell density in the gut mucosa of IBD patients corresponds to a reciprocal impairment in the Treg population. Taking in consideration all these positive and negative regulators of Treg cells, we derive the following equation:

$$\frac{dT_r}{dt} = \underbrace{\left[\left(\sigma_\beta\frac{I_\beta}{\zeta_\beta+I_\beta} + \sigma_{10}\frac{I_{10}}{\zeta_{10}+I_{10}}\right)\frac{I_2}{\zeta_2+I_2}\frac{M}{1+I_\alpha/\zeta_\alpha}\right]}_{\text{Cytokine signaling}}\underbrace{\left(\frac{1}{1+T_{17}/\gamma_{17}}\right)}_{\text{Inhibition by Th17}} - \underbrace{\mu_r T_r}_{\text{Decay}}. \quad (15)$$

Parameter estimation

Macrophages. We assumed that under normal conditions majority of gut macrophages display an M2 like phenotype. The parameters $\sigma_{M\gamma}$, σ_{M10}, $\sigma_{M\beta}$ and $\sigma_{M\alpha}$ represent the macrophage activation related coefficients under the influence of IFN-γ, IL-10, TGF-β and TNF-α cytokines, respectively. Given the assumption that under normal conditions M2 concentration is usually higher than M1, the activation rate of M2 is higher than that of M1; we arbitrarily

take $\sigma_{M10} = 10\sigma_{M\alpha}$. We also considered that the transition rates between M1 and M2 phenotypes are the same as the activation rate of M2, and take $\sigma_{M\beta} = \sigma_{M10}$ and $\sigma_{M\gamma} = \sigma_{M10}$.

Cytokines.   Th1 cells in the inflamed gut likely produce much more IFN-γ than macrophages. Thus we empirically considered the IFN-γ production rate in Th1 cells compared to that of macrophages, to be $v_{\gamma 1} = 5v_{\gamma M}$. We also assumed a similar production rate of IL-2 (v_{21}) and IFN-γ ($v_{\gamma 1}$) by Th1 cells, so that $v_{21} = v_{\gamma 1}$.

It was previously shown that Th2 cells at a density of 3×10^{-2} g/cm^3 produce an IL-4 concentration of 15×10^{-9} g/cm^3 [31]. Given $\delta_4 = 349.37$ week^{-1} [7, 32] and using the steady-state equation (this is expressed as $v_{42}T_2 - \delta_4 I_4 = 0$), we get $v_{42} = 1.75 \times 10^{-4}$ week^{-1}. We further assumed that Th2 cells produce more IL-4 than macrophages, and take $v_{4M} = v_{42}/3 = 5.83 \times 10^{-5}$ week^{-1}.

Mouse models of colitis have indicated that T cell derived IL-10 plays a more important role than the innate immune pool. We assumed that Treg cells produce more IL-10 than macrophages, and we took the IL-10 production rates to be $v_{10M} = 3.72 \times 10^{-4}$ week^{-1} [29, 33] and $v_{10r} = 3v_{10M}$.

T cells.   Maintenance of Th1 cells pool would require the activation and decay coefficients to be of similar magnitude. The coefficient σ_2 (representing the IL-2 maximal signal output) was estimated to be 1.23 week^{-1} while μ_1 (Th1 degradation rate coefficient) was 1.4 week^{-1}.

According to [34], we assume that Th17 activation rates by IL-6 is the same as that by IL-21, so that $\sigma_6 = \sigma_{21}$. Similarly, IL-10 and TGF-β contributions to Treg activation/survival rate were taken to be of equal magnitude, so that $\sigma_{10} = \sigma_\beta$.

Other parameters.   We take the inhibition of Th2 by Th1 to be $\gamma_1 = 1.83 \times 10^{-1}$ g/cm^3, the inhibition of Treg by Th17 to be $\gamma_{17} = 3.37 \times 10^{-1}$ g/cm^3, and assume that the inhibition of Th1 by Th2 is larger, taking $\gamma_2 = 5.35 \times 10^{-2}$ g/cm^3. We also assume that Treg inhibition effect on the other T cells is still somewhat larger, taking $\gamma_{r1} = \gamma_{r2} = \gamma_{r17} = 6.06 \times 10^{-2}$ g/cm^3.

From the data described in the section Data collection and analysis we obtained, in particular, the mRNA concentrations of TNF-α, IL-6 and IL-10 for healthy individuals as well as the master regulators of T cells for healthy individuals. The cytokine concentrations of TNF-α, IL-6 and IL-10 are assumed to be proportional to those of the mRNA concentration, with proportionality parameter λ_c. In [29], the cytokine concentrations are within 10^{-5}–10^{-9}g/cm^3; we take the IL-6 concentration in healthy tissue to be 8.00×10^{-6} g/cm^3. We can then compute λ_c and then also the concentrations of TNF-α, IL-10 in healthy tissue. We accordingly get the steady-state concentration of TNF-α to be 9.75×10^{-6} g/cm^3 and of IL-10 to be 1.54×10^{-6} g/cm^3.

The densities of Th1, Th2, Th17 and Treg in healthy tissue are assumed to be proportional to the concentrations of their master regulators with proportionality parameter λ_T which needs to be determined; the master regulators are obtained from the mRNA analysis described in the section Data collection and analysis. In addition to λ_T, there are still six important parameters that need to be determined, namely, v_{6M}, $v_{\alpha 1}$, σ_{12}, σ_4, σ_{21} and σ_β. We determine these 7 parameters as follows:

We assume that each half-saturation constant is the same as the steady state and solve the 15 steady-state equations of the system (1)-(15) for the following 15 variables: the 7 parameters defined above, and the 8 steady-state concentrations of IL-2, IL-4, IL-12, IL-21, TGF-β, IFN-γ, M1 macrophages and M2 macrophages.

Solving the steady-state system of 15 algebraic equations, we get the values of the parameters v_{6M}, $v_{\alpha 1}$, σ_{12}, σ_4, σ_{21} and σ_β (as shown in Tables 2 and 3 under "estimated from data"), and the steady-state concentrations of IL-2, IL-4, IL-12, IL-21, TGF-β, IFN-γ, M1 macrophages and M2 macrophages (shown in Table 4). Here we use the fact that the steady-state concentrations of λ_TTh1, λ_TTh2, λ_TTh17 and λ_TTreg are known from the analysis of the section Data collection and analysis. The half-saturation parameters are listed at the end of Table 3.

Table 2. Parameters used in the equations of macrophages and cytokines.

Parameter	Definition	Value	References
Macrophages			
f_1	Basal activation rate of M1	1 week^{-1}	[29] & estimated
f_2	Basal activation rate of M2	10 week^{-1}	[29] & estimated
$\sigma_{M\alpha}$	Activation rate of macrophages by TNF-α	2.4 week^{-1}	[29]
$\sigma_{M\gamma}$	Transition rate from M2 to M1	24 week^{-1}	[29] & estimated
σ_{M10}	Activation rate of macrophages by IL-10	24 week^{-1}	[29] & estimated
$\sigma_{M\beta}$	Transition rate from M1 to M2	24 week^{-1}	[29] & estimated
M_0	Density of inactivated macrophages	1.5 x 10^{-3} g/cm^3	[29, 35]
μ_M	Decay rate of macrophages	1 week^{-1}	[36]
Cytokines			
$v_{\gamma M}$	Production rate of IFN-γ by macrophages	8.2 x 10^{-6} week^{-1}	[29, 36]
$v_{\gamma 1}$	Production rate of IFN-γ by Th1	4.1 x10^{-5} week^{-1}	[29, 36] & estimated
v_{4M}	Production rate of IL-4 by macrophages	5.83 x10^{-5} week^{-1}	[31] & estimated
v_{42}	Production rate of IL-4 by Th2	1.75 x 10^{-4} week^{-1}	[31] & estimated
v_{6M}	Production rate of IL-6 by macrophages	3.63 x 10^{-3} week^{-1}	Estimated from data
v_{10M}	Production rate of IL-10 by macrophages	3.72 x 10^{-4} week^{-1}	[29, 33]
v_{10r}	Production rate of IL-10 by Treg	1.12 x 10^{-3} week^{-1}	[33] & estimated
v_{12M}	Production rate of IL-12 by macrophages	2.65 x 10^{-4} week^{-1}	[29, 36]
v_{2117}	Production rate of IL-21 by Th17	8.05 x 10^{-4} week^{-1}	[15]
$v_{\alpha M}$	Production rate of TNF-α by macrophages	2.10 x 10^{-2} week^{-1}	[29]
$v_{\alpha 1}$	Production rate of TNF-α by Th1	7.35 x 10^{-2} week^{-1}	Estimated from data
$v_{\beta M}$	Production rate of TGF-β by macrophages	5.6 x 10^{-9} week^{-1}	[29]
$v_{\beta r}$	Production rate of TGF-β by Treg	3.90 x 10^{-8} week^{-1}	[37]
v_{21}	Production rate of IL-2 by Th1	4.1 x 10^{-5} week^{-1}	[29, 36] & estimated
n_{2r}	Production ratio of IL-10 by IL-2	3	Estimated
δ_γ	Degradation rate of IFN-γ	29.12 week^{-1}	[7, 18]
δ_4	Degradation rate of IL-4	349.37 week^{-1}	[7, 32]
δ_6	Degradation rate of IL-6	29.11 week^{-1}	[38]
δ_{10}	Degradation rate of IL-10	116.48 week^{-1}	[39]
δ_{12}	Degradation rate of IL-12	8.33 week^{-1}	[29]
δ_{21}	Degradation rate of IL-21	63.98 week^{-1}	[40]
δ_α	Degradation rate of TNF-α	388.15 week^{-1}	[41]
δ_β	Degradation rate of TGF-β	349.37 week^{-1}	[7, 42]
δ_2	Degradation rate of IL-2	537.46 week^{-1}	[7, 43]

doi:10.1371/journal.pone.0165782.t002

For completeness we listed in Table 4 all the steady-state concentrations of cytokines, macrophages and T cells; this list partially overlaps with Table 3.

Parameter sensitivity analysis

Since the model is highly complicated with a lot of parameters and some parameters are estimated roughly from data, we performed sensitivity analysis to determine the robustness of the simulation results and effect of the parameters on the concentrations of Th1 and Th2 cells which are used to determine the types of IBD patients. In our parameter analysis, we focused on nine parameters, $\sigma_{M\alpha}$, σ_{M10}, σ_{12}, σ_2, σ_4 σ_{21}, σ_6, σ_β and σ_{10}, which are the activation rates of macrophages and T cells by different types of cytokines and are the most significant in the disease dynamics.

Table 3. Parameters used in the equations of T cells and a list of half-saturation constants.

Parameter	Definition	Value	References
T cells			
μ_1	Decay rate of Th1	1.4 week^{-1}	[29, 36]
μ_2	Decay rate of Th2	1.4 week^{-1}	[29, 36]
μ_{17}	Decay rate of Th17	1.4 week^{-1}	[29, 36]
μ_r	Decay rate of Treg	1.4 week^{-1}	[29, 36]
σ_{12}	Maximum rate of IL-12 signaling	10.93 week^{-1}	Estimated from data
σ_2	Maximum rate of IL-2 signaling	1.23 week^{-1}	[29, 36] & estimated
σ_4	Maximum rate of IL-4 signaling	1.94 week^{-1}	Estimated from data
σ_{21}	Maximum rate of IL-21 signaling	156.17 week^{-1}	[34] & estimated from data
σ_6	Maximum rate of IL-6 signaling	156.17 week^{-1}	[34] & estimated from data
σ_β	Maximum rate of TGF-β signaling	14.02 week^{-1}	Estimated from data
σ_{10}	Maximum rate of IL-10 signaling	14.02 week^{-1}	Estimated from data
γ_1	Constants for Th1 inhibition of Th2	1.83×10^{-1} g/cm^3	Estimated
γ_2	Constants for Th2 inhibition of Th1	5.35×10^{-2} g/cm^3	Estimated
$\gamma_{r1}, \gamma_{r2}, \gamma_{r17}$	Constants for Treg inhibition	6.06×10^{-2} g/cm^3	Estimated
γ_{17}	Constants for Th17 inhibition	3.37×10^{-1} g/cm^3	Estimated
Half-saturation constants			
ζ_6	Constant for IL-6	8×10^{-6} g/cm^3	The constants are the same as the steady-state concentrations of the cytokines in healthy individuals; in solving for the steady-state equations of (1)-(15)
ζ_α	Constant for TNF-α	9.75×10^{-6} g/cm^3	
ζ_{10}	Constant for Il-10	1.54×10^{-6} g/cm^3	
ζ_2	Constant for IL-2	6.86×10^{-8} g/cm^3	
ζ_γ	Constant for IFN-γ	2.58×10^{-6} g/cm^3	
ζ_{12}	Constant for IL-12	4.90×10^{-8} g/cm^3	
ζ_4	Constant for IL-4	9.70×10^{-9} g/cm^3	
ζ_{21}	Constant for IL-21	4.25×10^{-6} g/cm^3	
ζ_β	Constant for TGF-β	6.77×10^{-12} g/cm^3	

We applied the method of Partial Rank Correlation Coefficient (PRCC) [44] for our sensitivity analysis. We ran 5000 simulations in which all the nine parameters are varied according to Latin hypercube sampling with the range of ±20% perturbation around the parameter values obtained for healthy individuals. The results of the sensitivity analysis are summarized in Table 5. Fig 2 shows the scatter plots of rank transformed T_1 (Fig 2A) and T_2 (Fig 2B) after 100 weeks (solution close to steady state) versus the rank transformed parameters with significant correlation (|PRCC|>0.5) and p-value (p<0.01); the title of each subplot shows its PRCC value.

All the nine parameters have significant PRCC values either with T_1 or with T_2. Among the nine parameters, we find that the statistically significant PRCC values with both T_1 and T_2 are σ_{12}, σ_β and σ_{10}. The parameters σ_β and σ_{10} are negatively correlated to T_1 and T_2: the two

Table 4. Steady-state concentrations of cytokines, macrophages and T cells in a healthy individual.

	Value (g/cm^3)
M1 macrophage	2.34 x 10^{-2}
M2 macrophage	2.50 x 10^{-2}
Th1 cell	4.58 x 10^{-2}
Th2 cell	1.34 x 10^{-2}
Th17 cell	3.37 x 10^{-1}
Treg cell	6.06 x 10^{-2}
IFN-γ	2.58 x 10^{-6}
IL-2	6.86 x 10^{-8}
IL-4	9.70 x 10^{-9}
IL-21	4.25 x 10^{-6}
IL-6	8.00 x 10^{-6}
TNF-α	9.75 x 10^{-6}
IL-10	1.54 x 10^{-6}
TGF-β	6.77x 10^{-12}
IL-12	4.90 x 10^{-8}

doi:10.1371/journal.pone.0165782.t004

parameters are the activation rates of Treg cells which inhibit Th1 and Th2 activations. This result is consistant with the observation that the abnormal levels of T cells usually arise from abnormal regulation of Th1 and Th2 cells by Treg cells [7]. On the other hand, σ_{12} is positively correlated to T_1 and T_2: as the parameter increases, the amount of Th1 cells increases and thus Treg cell regulation on Th1 and Th2 cells decreases through increased TNF-α inhibtion produced by Th1 cells. Note that although Th1 and Th2 cells inhibit each other, reduced Treg inhibtion has a larger effect than the mutual inihbition between Th1 and Th2 cells. The roles of these three parameters (σ_{12}, σ_β and σ_{10}) on different types of IBD will be discussed in the Result section later.

Data collection and analysis

Human subjects and tissue biopsy collection. Colon biopsies from healthy controls and patients with Inflammatory Bowel Diseases were obtained from a de-identified tissue bank. The tissue bank is Host Modifiers of Inflammatory Bowel Diseases Phenotypes and IRB protocol number is 06-0270-F1V. The Institutional Review Board at the University of Kentucky

Table 5. PRCC values of some parameters for the outputs T_1 and T_2.

	PRCC for T_1	PRCC for T_2
$\sigma_{M\alpha}$	0.3298*	-0.0190
σ_{M10}	0.6264*	-0.1448*
σ_{12}	0.6206*	0.8420*
σ_2	0.2257*	0.4404*
σ_4	-0.3123*	-0.4336*
σ_{21}	0.2756*	0.3192*
σ_6	0.4181*	0.4954*
σ_β	-0.6690*	-0.7636*
σ_{10}	-0.6866*	-0.7858*

* Denotes significant PRCC values (p-value <0.01).

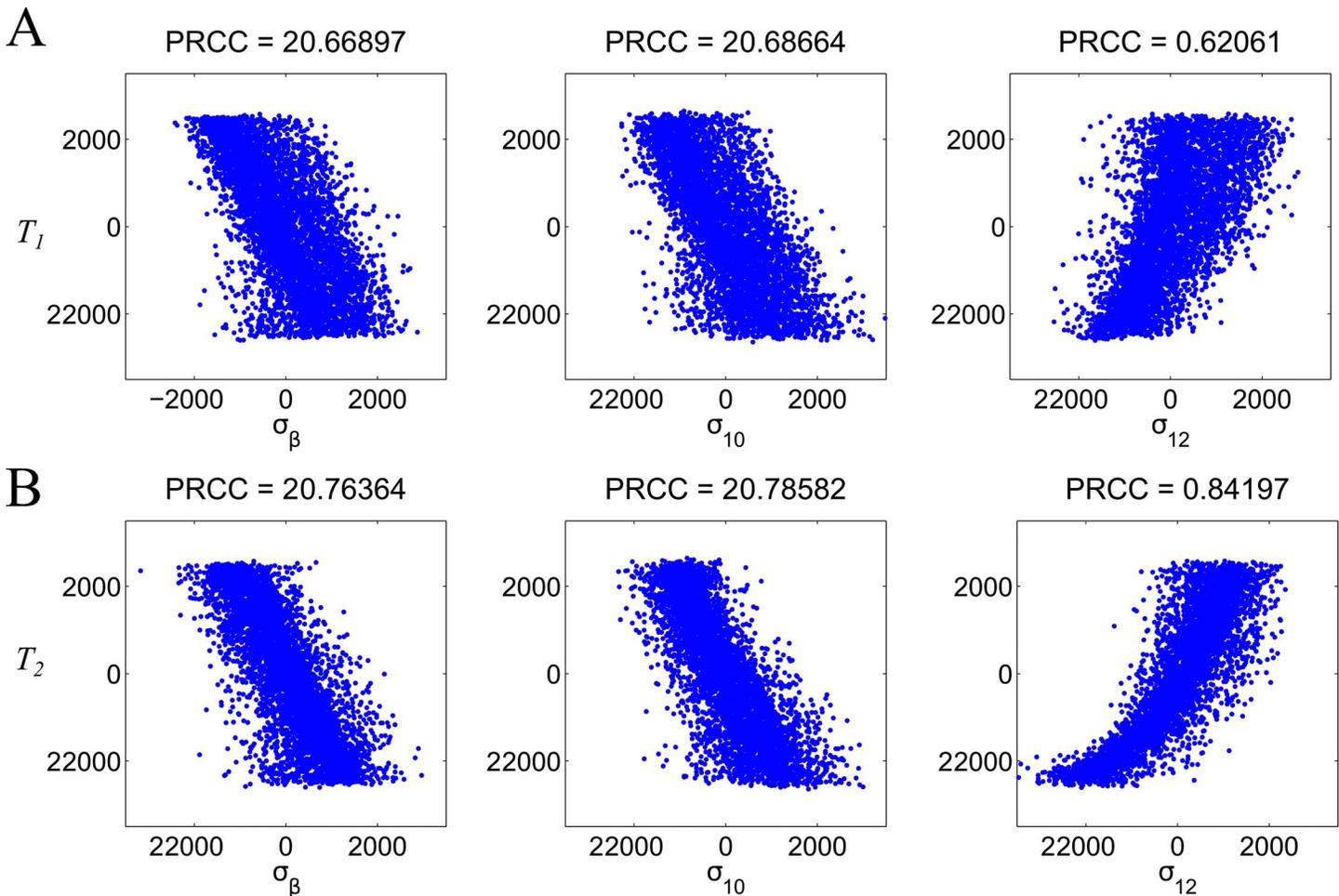doi:10.1371/journal.pone.0165782.t005

Fig 2. Scatter plots of rank transformed T_1 (A) and T_2 (B) after 100 weeks versus some rank transformed parameters with statistically significant correlation (|PRCC|>0.5 and p-value <0.01). The title of each subplot shows its PRCC value.

approved the tissue bank protocol. Banked, normal biopsies were obtained from healthy controls that underwent screening colonoscopy. IBD patients had an established diagnosis of Crohn's disease involving the colon and were off immunosuppressant treatment at the time of the endoscopic procedure. Biopsies were obtained inflamed but not ulcerated colonic mucosa. All measures were derived from mucosal biopsies. No blood samples were utilized in our experiment. Patient characteristics are shown in Table 6.

Cytokine profile data tends to be affected by the contamination of epithelial cells that cannot produce typical Th1/Th2 cytokines. Nevertheless all biopsies are expected to have a similar content of epithelial cells: we used the same standard biopsies forceps, applied en-face orientation, and for all IBD patients the biopsy was performed at the area abutting ulceration. If anything, biopsies from IBD patients would have been expected to contain less epithelial cells, due to surface erosion. Since control and IBD biopsies contained epithelial cells the differences in immune markers are expected to be representative of the inflammatory process.

mRNA analysis. Frozen biopsies were placed in 600μl lysis buffer (MagNA Pure Compact RNA Isolation Kit) at room temperature for 10 min. Biopsies were disrupted using a MagNA Lyser instrument (Roche, Basel Switzerland) and beads: 1st spin @ 7000x for 40 sec and 2nd spin @6000x for 30 sec. Tubes were placed in the instrument cooling block for 15 min and then

Table 6. Baseline characteristics for patients with IBD-Crohn's Disease.

Total number	N = 58
Gender	
Female	27(46.55%)
Male	31(53.45%)
Location	
Upper GI	0(0%)
Ileal	0(0%)
Ileo-colonic	47(81.03%)
Colonic	11(18.97%)
Perianal	6(10.34%)
Behavior	
Inflammatory	41(70.68%)
Stricturing	14(24.13%)
Fistulizing	3(5.17%)
Current immunosuppressant treatment	0(0%)
Former use of immunomodulator	27(46.55%)
Former use of biologic therapy	19(32.75%)

doi:10.1371/journal.pone.0165782.t006

centrifuged briefly to pellet the debris. The supernatant containing total RNA was then purified by MagNA Pure Compact RNA Isolation Kit (Roche) protocol with elution volume of 50ul. For control RNA quality and quantity were determined with a spectrophotometer (NanoDrop Technologices, Wilmington, DE).

Gene expression analysis. Total mRNA (15μl) were analyzed using the nCounter Master Kit from NanoString Technologies (NanoString Technologies, Inc Seattle, WA). Gene Expression CodeSets of our interest for the nCounter Analysis System were preordered from Nano-String Technologies, Inc (www.nanostring.com). The nCounter Analysis System is an integrated system comprised of a fully-automated Prep Station, a Digital Analyzer, and the CodeSet (molecular barcodes) reader.

Results

In the sequel we shall use the following abbreviations:

T_{1ssh}: the mean value of the Th1 master regulator T-bet of healthy individuals

T_{1ss}: the value of the Th1 master regulator T-bet of IBD patient

T_{2ssh}: the mean value of the Th2 master regulator GATA-3 of healthy individuals

T_{2ss}: the value of the Th2 master regulator GATA-3 of IBD patient

We obtained gut mucosal samples from healthy individuals and IBD-Crohn's patients and measured the mRNA expression for cytokines IL-6, IL-10, TNF-α and transcription factors T-bet, GATA3, RORγt and Foxp3. Based on the observed values we were able to divide the patients into four categories:

Type 1. $T_{1ss} > T_{1ssh}$, $T_{2ss} < T_{2ssh}$

Type 2. $T_{1ss} < T_{1ssh}$, $T_{2ss} > T_{2ssh}$

Type 3. $T_{1ss} > T_{1ssh}$, $T_{2ss} > T_{2ssh}$

Table 7. Fold changes of the cytokine and T cell concentrations obtained from the clinical data and the simulations in different types of diseases.

Type of diseases	# of cases	IL-6	IL-10	TNF-α	T-Bet	Gata3	RORγt	Foxp3	TGF-β*	IFN-γ*
Th1↑ Th2↓	7	↓-93%	↓-51%	↓-31%	↑+50%	↓-22%	↑+50%	↓-71%	↓-56%	↓-99%
Th1↓Th2↑	18	↓-74%	↓-15%	↓-31%	↓-29%	↑+50%	↓-27%	↑+1%	↓-6%	↓-92%
Th1↓Th2↑	18	↓-74%	↓-15%	↓-31%	↓-29%	↑+50%	↓-27%	↑+1%	↓-6%	↓-92%
Th1↑Th2↑	17	↑+35%	↑+44%	↑+47%	↑+110%	↑+75%	↓-14%	↑+70%	↑+19%	↑+481%
Th1↓Th2↓	16	↓-83%	↓-34%	↓-45%	↓-46%	↓-40%	↓-11%	↓-42%	↓-20%	↓-95%

* The values of TGF-β and IFN-γ are predicted by the model.

Type 4. $T_{1ss} < T_{1ssh}$, $T_{2ss} < T_{2ssh}$

For example, if an IBD patient had a T-bet level higher than T_{1ssh} and a GATA-3 level lower than T_{2ssh}, this patient is classified to Type 1 group. There are totally 58 patients: 7 in Type 1, 18 in Type 2, 17 in Type 3 and 16 in Type 4. The deviations of mRNA fold expression of IBD patients from healthy individuals are shown in Table 7.

Our next step was to determine the values of coefficients that define the production rate of individual cytokines and activation of master regulators. These theoretical parameter variations (cytokine production, T cell activation), in each of the four types, were determined using the steady-state solution of our mathematical model and are shown in Table 7. We assumed that the blood sample data reflect the tissue data (by the same proportionality parameter), and that the disease state occurred at the steady state when some of the production/activation rates related to T cells were deregulated, either increased or decreased. Here we consider the variations of the following parameters, v_{g1}, $v_{\alpha1}$, $v_{\beta r}$, v_{10r}, σ_{12}, σ_4, σ_{21}, σ_6, σ_β and σ_{10} (Table 8).

In type 1 group the production rate of Th1 cytokines, IFN-γ and TNF-α, was decreased while the anti-inflammatory IL-10 was increased. Nevertheless the signal strength of IL-12, IL-21 and IL-6 favored activation of Th1 and Th17 pathways. On the other hand, decreased activation of Treg by TGF-β and IL-10 was able to offset their increased production rate.

In type 2 group, despite an increase in TNF-α production rate and IL-12 signal strength, the lack of IL-21 and IL-6 signal strength coupled with increased IL-4 signal strength tipped the balance in favor of Th2 response.

Type 3 group was the only one with a robust IFN-γ production rate. Interestingly we no longer observed the reciprocity between the Th1, Th2, Th17 and Treg activation rates, as the signal strength for IL-12, IL-4, IL-21, IL-6, TGF-β and IL-10 were increased across the board.

Type 4 group was characterized by a global decrease in signal strength and thus lack of T cell activation even though this group had the highest production rate of TNF-α

Table 8. Simulation results: Parameter variations in different types of diseases.

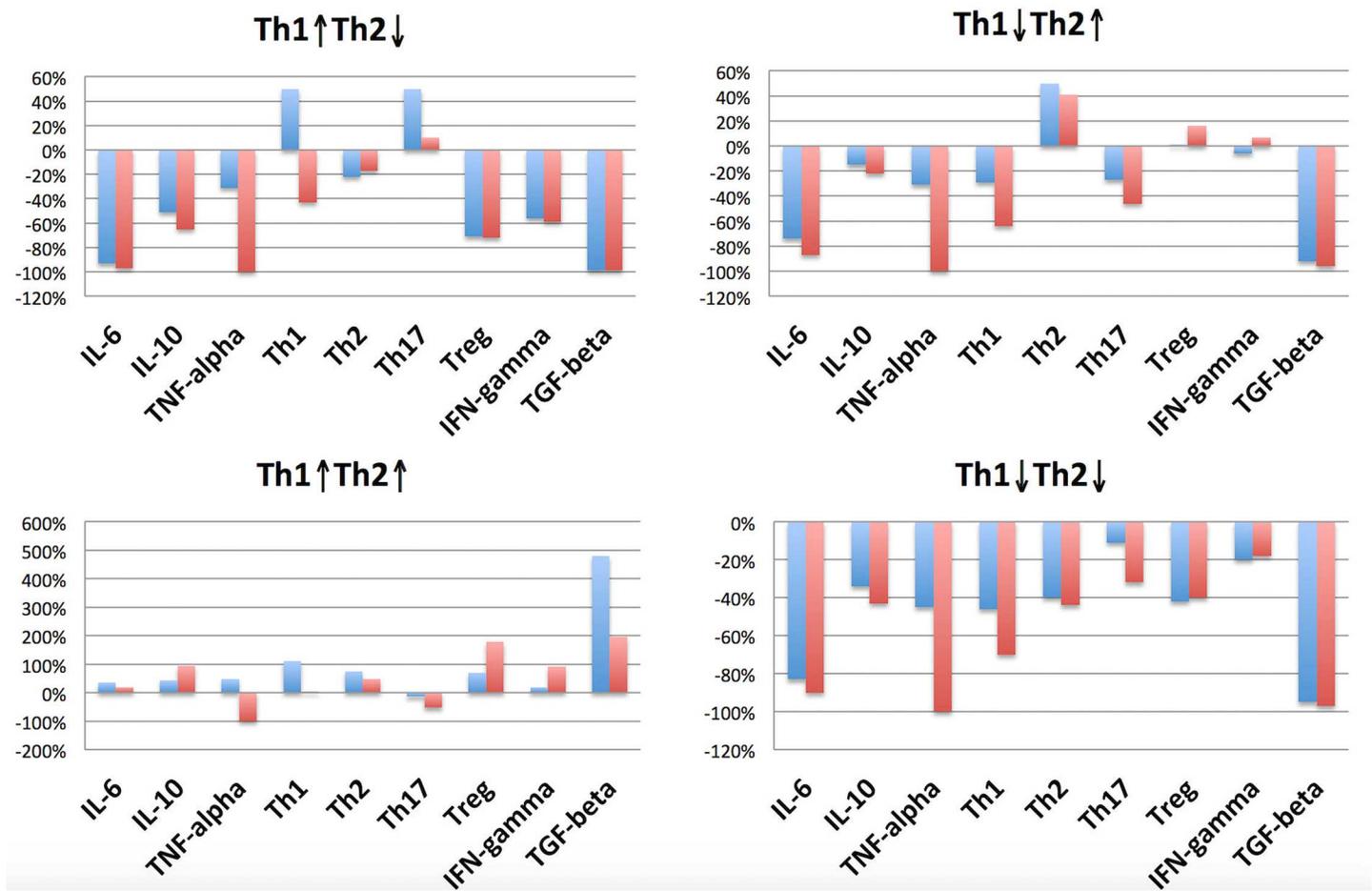| Type of diseases	$v_{\gamma1}$ coefficient of IFN-γ by Th1	$v_{\alpha1}$ coefficient of TNF-α by Th1	$v_{\beta\rho}$ coefficient of TGF-β by Treg	$v_{10\rho}$ coefficient of IL-10 by Treg	σ_{12} activation of Th1 cells	σ_4 activation of Th2 cells	σ_{21} activation of Th17 cells	σ_6 activation of Th17 cells	σ_β activation of Treg cells	σ_{10} activation of Treg cells
Th1↑Th2↓	↓-99.6%	↓-50%	↑+35%	↑+35%	↑+298%	↓-32%	↑+49%	↑+49%	↓-50%	↓-50%
Th1↓Th2↑	↓-90%	↑+4%	↓-10%	↓-10%	↑+81%	↑+25%	↓-13%	↓-13%	-0%	-0%
Th1↑Th2↑	↑+194%	↓-29%	↓-30%	↓-30%	↑+255%	↑+122%	↑+298%	↑+298%	↑+17%	↑+17%
Th1↓Th2↓	↓-92%	↑+11%	↑+32%	↑+32%	↑+5%	↓-48%	↓-28%	↓-28%	↓-18%	↓-18%

Fig 3. Simulation results: fold changes of the cytokine and T cell concentrations when TNF-α is completely blocked in different types of diseases. Blue bars represent the results of pre-treatment; red bars represent the results of post-treatment with TNF-α blockage.

Currently, anti-TNF antibodies represent the main group of biologic agents for the treatment of IBD. Therefore we simulated the TNF-α blockade in our mathematical model. For modeling the TNF-α blockade, we fix the concentration of TNF-α (I_α) to be zero and calculate the change of other variables at the steady-state concentrations. Fig 3 shows the predicted mRNA fold change in cytokines and T cell master regulators. In type 1 group, TNF-α blockade had the most profound effect on Th1 (93%) and Th17 (40%) master regulators. In the third group our model predicted a significant decrease in Th1 (105%) and increase in Treg (108%). In the second and fourth group the decrease in both Th1 (35%, 34%) and Th17 (19%, 21%) master regulators was modest whereas Treg was virtually unaffected (1%, 2%).

Conclusions and Discussion

Inflammatory Bowel Diseases are characterized by a deregulated immune response toward gut microbiota. A simplistic characterization of disease phenotype divides patients into either Crohn's Disease or Ulcerative Colitis. Nevertheless, if we take into account the individual variations in genetic background, microbiome, environmental exposure, nutrition, and life-style, we can foresee multiple immune phenotypes. The development of current biological therapies in CD mirrors our understanding of immune regulatory pathways. Current Montreal

classification distinguishes phenotypes based on anatomical and clinical criteria. Unfortunately this will not help identify individual immune phenotype relevant to a particular biologic treatment. Pretreatment knowledge of the relevant gut mucosal immune dysfunction in a given patient would significantly improve the risk/benefit balance and open the way toward personalized medical care.

Patients with inflammatory bowel diseases have elevated levels of circulating and gut mucosal cytokines [1]. Downstream signaling from these inflammatory mediators, activate transcription factors T-bet, GATA3, Foxp3 and RORγt [3]. A complex network of regulatory feedback loops involving these cytokines and their targets, are responsible for the polarization of naïve T cells into specific T helper cells: Th1, Th2, Th17 and Treg [3, 4].

In this study we developed a mathematical model of differential equations to describe immune regulatory pathways in patients with CD. The output of these differential equations was dependent on the relative mRNA expression of specific immune system targets.

Patient stratification based on calculated Th1 and Th2 immune cell activation, relative to healthy controls, identified 4 distinct immune phenotypes. These were further characterized based on cytokine production as well as the mRNA expression of the Th1/Th2/Th17 and Treg master regulators.

While it is tempting to analyze individual cytokines when predicting response to a particular biological treatment, the overall immune response is a resultant of opposing factors. The relative magnitude of the end state compared to healthy controls or pre/post treatment status may offer a way to predict response to a particular biologic treatment. We performed an *in-silico* simulation of TNF-α blockade for each of the 4 immune phenotypes identified by our mathematical algorithm. Globally the largest impact was seen in type 3 group (Th1^{high}/Th2^{high}) where a diminished Th1 and Th17 activation was predicted along with a reciprocal increase in Treg and TGF-β. Therefore this group appeared to have the best immunologic outcome by blocking the TNF-α. Our findings through mathematical modeling mirror the observations in patients with IBD, where Infliximab treatment down-regulates IL-17 expression in the gut mucosa and promotes healing [45]. On the other hand, type 4 was more consistent with a global immunosuppressed status, and anti-TNF blockade further magnified this changes relative to healthy controls. Our study included samples from symptomatic and/or with evidence of disease activity (abnormal CRP, Calprotectin, anemia) CD patients. All patients were off immunosuppressive therapy at the time of endoscopy for at least 3 month. 8 (50%) of type 4 group patients had previously experienced a failure to at least one biologic treatment. Thus type 4 group (Th1^{Low}/Th2^{Low}) should be a candidate for immune stimulatory therapy rather than further immunosuppression. Also, importantly, the paradoxical presence of clinical and endoscopic activity in this group underscores the importance of global analysis rather than individual immune mediator analysis. In conclusion we propose that mathematical modeling of immune regulatory networks in patients with IBD may allow identifying distinct groups with high relevance to biological therapies. Based on the results of the in-silico simulation of TNF blockade, a multi-pronged approach aimed at several distinct pathways might be superior to biologic monotherapy. In certain cases (type 4) immune activation rather than suppression might be recommended.

Although parameters (coefficients for differential equations) were obtained from other models, they are representative of a chronic inflammatory process and thus relevant to IBD. Sarcoidosis and Lupus (models referenced in our study) also share genetic susceptibility loci with Crohn's disease. Ultimately, validation and refinement of the mathematical parameters will require a prospective approach in IBD patients. Our current model is supposed to provide a basis for such future studies.

We acknowledge that more cytokines could have been included in the present study. Coefficients utilized in the present mathematical model were also derived from prior models of inflammation, which did not include IL-5, IL-13, IL-17 and IL-22. Naïve T helper cells can be induced to differentiate towards T helper 1 (Th1), Th2, Th17 and regulatory (Treg) phenotypes according to the local cytokine milieu. Stable expression of specific transcription factors, T-bet (Th1), GATA-3 (Th2), Foxp3 (Tregs) and RORγt (Th17) will ultimately represent the net effect of the combine cytokine production. Thus the inclusion of all the master regulators relevant to the T cell polarization is expected to reflect the tissue status of these pathways. This potential extension of the modeling with inclusion of the extra cytokines should be considered in future work when more patients data become available.

Our present study represents a snapshot of CD patients evaluated for assessment of disease activity. We intentionally excluded patients with recent exposure to immunosuppressant therapy to avoid a direct influence of the chosen markers. Nevertheless the purpose of the current study was to establish a mathematical model based on IBD patient samples that will serve as a basis for prospective studies.

Acknowledgments

Author Contributions

Conceptualization: WCL AF RA.

Data curation: WCL RA.

Formal analysis: WCL RA.

Funding acquisition: WCL AF.

Investigation: WCL, RA.

Methodology: WCL RA.

Project administration: WCL AF.

Resources: RA VA.

Software: WCL.

Supervision: AF.

Validation: WCL RA.

Visualization: WCL.

Writing – original draft: WCL AF RA.

Writing – review & editing: WCL AF.

References

1. Shim JO. Gut Microbiota in inflammatory bowel disease. Pediatr Gastroenterol Hepatol Nutr. 2013; 16 (1): 17–21. doi: 10.5223/pghn.2013.16.1.17 PMID: 24010101

2. Mesbah-Uddin M, Elango R, Banaganapalli B, Shaik NA, Al-Abbasi FA. In-silico analysis of inflammatory bowel disease (IBD) GWAS loci to novel connections. PLoS One. 2015; 10(3): e0119420. doi: 10.1371/journal.pone.0119420 PMID: 25786114

3. Targan SR, Shih DQ. Insights into IBD pathogenesis. Curr Gastroenterol. Rep. 2009; 11(6): 473–480. PMID: 19903423

4. Zenewicz LA, Antov A, Flavell RA. CD4 T-cell differentiation and inflammatory bowel disease. Trends Mol Med. 2009; 15(5): 199–207. doi: 10.1016/j.molmed.2009.03.002 PMID: 19362058

5. Mizoguchi A, Mizoguchi E. Animal models of IBD: linkage to human disease. Curr Opin Pharmacol. 2010; 10(5): 578–87. doi: 10.1016/j.coph.2010.05.007 PMID: 20860919

6. Satsangi J, Silverberg MS, Vermeire S, Colombel JF. The Montreal classification of inflammatory bowel disease: controversies, consensus, and implications. Gut. 2006; 55(6): 749–753. doi: 10.1136/gut.2005.082909 PMID: 16698746

7. Lo WC, Arsenescu RI, Friedman A. Mathematical model of the roles of T cells in inflammatory bowel disease. Bull Math Biol. 2013; 75(9): 1417–33. doi: 10.1007/s11538-013-9853-2 PMID: 23760658

8. Bettelli E, Carrier Y, Gao W, Korn T, Strom TB, Oukka M, et al. Reciprocal developmental pathways for the generation of pathogenic effector TH17 and regulatory T cells. Nature. 2006; 441(7090): 235–238. doi: 10.1038/nature04753 PMID: 16648838

9. Hong T, Xing J, Li L, Tyson JJ. A mathematical model for the reciprocal differentiation of T helper 17 cells and induced regulatory T cells. PLoS Comput Biol. 2011; 7(7): e1002122. doi: 10.1371/journal.pcbi.1002122 PMID: 21829337

10. Maloy K, Powrie F. Intestinal homeostasis and its breakdown in inflammatory bowel disease. Nature. 2011; 474(7351): 298–306. doi: 10.1038/nature10208 PMID: 21677746

11. Hwang ES, Hong JH, Glimcher LH. IL-2 production in developing Th1 cells is regulated by heterodimerization of RelA and T-bet and requires T-bet serine residue 508. J Exp Med. 2005; 202: 1289–1300. doi: 10.1084/jem.20051044 PMID: 16275766

12. Osugi Y, Hara J, Tagawa S, Takai K, Hosoi G, Matsuda Y, et al. Cytokine production regulating Th1 and Th2 cytokines in hemophagocytic lymphohistiocytosis. Blood. 1997; 89: 4100–4103. PMID: 9166851

13. Baumgart DC, Carding SR. Inflammatory bowel disease: cause and immunobiology. Lancet. 2007; 369(9573): 1627–1640. doi: 10.1016/S0140-6736(07)60750-8 PMID: 17499605

14. Murphy KM, Stockinger B. Effector T cell plasticity: flexibility in the face of changing circumstances. Nat Immunol. 2010; 11(8): 674–680. doi: 10.1038/ni.1899 PMID: 20644573

15. Wei L, Laurence A, Elias KM, O'Shea JJ. IL-21 is produced by Th17 cells and drives IL-17 production in a STAT3-dependent manner. J Biol Chem. 2007; 282(48): 34605–34610. doi: 10.1074/jbc.M705100200 PMID: 17884812

16. Zhang J, Patel MB, Griffiths R, Mao A, Song YS, Karlovich NS, et al. Tumor Necrosis Factor-alpha Produced in the Kidney Contributes to Angiotensin II-dependent Hypertension. Hypertension. 2014; 64(6): 1275–81. doi: 10.1161/HYPERTENSIONAHA.114.03863 PMID: 25185128

17. Chaudhry A, Samstein RM, Treuting P, Liang Y, Pils MC, Heinrich JM, et al. Interleukin-10 signaling in regulatory T cells is required for suppression of Th17 cell-mediated inflammation. Immunity. 2011; 34 (4): 566–578. doi: 10.1016/j.immuni.2011.03.018 PMID: 21511185

18. Grassegger A, Hopf R. Significance of the cytokine interferon gamma in clinical dermatology, Clin Exp Dermatol. 2004; 29:584–588. doi: 10.1111/j.1365-2230.2004.01652.x PMID: 15550127

19. D'Andrea A, Aste-Amezaga M, Valiante NM, Ma X, Kubin M, Trinchieri G. Interleukin 10 (IL-10) inhibits human lymphocyte interferon gamma-production by suppressing natural killer cell stimulatory factor/IL-12 synthesis in accessory cells. J Exp Med. 1993; 178(3):1041–1048. PMID: 8102388

20. Pueringer RJ, Schwartz DA, Dayton CS, Gilbert SR, Hunninghake GW. The relationship between alveolar macrophage TNF, IL-1, and PGE2 release, alveolitis, and disease severity in sarcoidosis. Chest. 1993; 103(3):832–838. PMID: 8449077

21. Matinez FO, Gordon S. The M1 and M2 paradigm of macrophage activation: time for reassessment. F1000Prime Rep. 2014; 6(13):6–13.

22. Wang Y, Yang T, Ma Y, Halade GV, Zhang J, Lindsey ML, Jin YF. Mathematical modeling and stability analysis of macrophage activation in left ventricular remodeling post-myocardial infarction. BMC Genomics. 2012; 13(6):S21.

23. Nelson BH. IL-2, regulatory T cells, and tolerance. J. Immunol. 2004; 172:3983–3988. PMID: 15034008

24. Stummvoll GH, DiPaolo RJ, Huter EN, Davidson TS, Glass D, Ward JM, et al. Th1, Th2, and Th17 effector T cell-induced autoimmune gastritis differs in pathological pattern and in susceptibility to suppression by regulatory T cells. J Immunol. 2008; 181(3):1908–1916. PMID: 18641328

25. Szabo SJ, Dighe AS, Gubler U, Murphy KM. Regulation of the interleukin (IL)-12R beta 2 subunit expression in developing T helper 1 (Th1) and Th2 cells. J Exp Med. 1997; 185(5):817–824. PMID: 9120387

26. Harrington LE, Mangan PR, Weaver CT. Expanding the effector CD4 T-cell repertoire: the Th17 lineage. Curr Opin Immunol. 2006; 18(3):349–356. doi: 10.1016/j.coi.2006.03.017 PMID: 16616472

27. Brooks DG, Walsh KB, Elsaesser H, Oldstone MBA. IL-10 directly suppresses CD4 but not CD8 T cell effector and memory responses following acute viral infection. Proc Natl Acad Sci U S A. 2010; 107 (7):3018–3023. doi: 10.1073/pnas.0914500107 PMID: 20133700

28. Viallard JF, Pellegrin JL, Ranchin V, Schaeverbeke T, Dehais J, Longy-Boursier M, et al. Th1 (IL-2, interferon-gamma (IFN-gamma)) and Th2 (IL-10, IL-4) cytokine production by peripheral blood mononuclear cells (PBMC) from patients with systemic lupus erythematosus (SLE). Clin Exp Immunol. 1999; 115(1):189–195. doi: 10.1046/j.1365-2249.1999.00766.x PMID: 9933441

29. Hao W, Crouser ED, Friedman A. A mathematical model of sarcoidosis. Proc Natl Acad Sci U S A. 2014; 111(45):16065–70. doi: 10.1073/pnas.1417789111 PMID: 25349384

30. Valencia X, Stephens G, Goldbach-Mansky R, Wilson M, Shevach EM, Lipsky PE. TNF downmodulates the function of human CD4+CD25hi T-regulatory cells. Blood. 2006; 108(1): 253–261. doi: 10.1182/blood-2005-11-4567 PMID: 16537805

31. Hu-Li J, Huang H, Ryan J and Paul WE. In differentiated CD4+ T cells, interleukin 4 production is cytokine-autonomous, whereas interferon gamma production is cytokine-dependent. Proc Natl Acad Sci U S A. 1997; 94(7):3189–3194. PMID: 9096368

32. Conlon PJ, Tyler S, Grabstein KH, Morrissey P. Interleukin-4 (B-cell stimulatory factor-1) augments the in vivo generation of cytotoxic cells in immunosuppressed animals. Biotechnol Ther. 1989; 1:31–41. PMID: 2562642

33. Toossi Z, Hirsch CS, Hamilton BD, Knuth CK, Friedlander MA, Rich EA. Decreased production of TGF-beta 1 by human alveolar macrophages compared with blood monocytes. J Immunol. 1996; 156 (9):3461–3468. PMID: 8617974

34. Coquet JM, Chakravarti S, Smyth MJ, Godfrey DI. Cutting edge: IL-21 is not essential for Th17 differentiation or experimental autoimmune encephalomyelitis. J Immunol. 2008; 180(11):7091–7101.

35. Wallace WA, Gillooly M, Lamb D. Intra-alveolar macrophage numbers in current smokers and non-smokers: a morphometric study of tissue sections. Thorax. 1992; 47(6):437–440. PMID: 1496503

36. Crouser ED, Culver DA, Knox KS, Julian MW, Shao G, Abraham S, et al. Gene expression profiling identifies MMP-12 and ADAMDEC1 as potential pathogenic mediators of pulmonary sarcoidosis. Am J Respir Crit Care Med. 2009; 179(10):929–938. doi: 10.1164/rccm.200803-490OC PMID: 19218196

37. Li MO, Wan YY, Flavell RA. T cell-produced transforming growth factor-beta1 controls T cell tolerance and regulates Th1- and Th17-cell differentiation. Immunity. 2007; 26(5):579–591. doi: 10.1016/j.immuni.2007.03.014 PMID: 17481928

38. Marino A,Giotta N. Cinacalcet, fetuin-A and interleukin-6. Nephrol Dial Transpl. 2008; 23(4):1460–1461.

39. Le T, Leung L, Carroll WL and Schibler KR. Regulation of interleukin-10 gene expression: possible mechanisms accounting for its upregulation and for maturational differences in its expression by blood mononuclear cells. Blood. 1997; 89(11):4112–4119. PMID: 9166853

40. Bhatia S, Curti B, Ernstoff MS, Gordon M, Heath EI, Miller WHJ, et al. Recombinant interleukin-21 plus sorafenib for metastatic renal cell carcinoma: a phase 1/2 study. J Immunother Cancer. 2014; 2:2. doi: 10.1186/2051-1426-2-2 PMID: 24829759

41. Oliver JC, Bland KA, Oettinger CW, Arduino MJ, McAllister SK, Aguero SM, et al. Cytokine kinetics in an in vitro whole blood model following an endotoxin challenge. Lymphokine Cytokine Res. 1993; 12 (2):115–120. PMID: 8324076

42. Kaminskam B, Wesolowska A and Danilkiewicz M. TGF beta signalling and its role in tumour pathogenesis. Acta Biochim Pol. 2005; 52:329–337. PMID: 15990918

43. Rao BM, Driver I, Lauffenburger DA and Wittrup KD. Interleukin 2 (IL-2) variants engineered for increased IL-2 receptor alpha-subunit affinity exhibit increased potency arising from a cell surface ligand reservoir effect. Mol Pharmacol. 2004; 66: 864–869. doi: 10.1124/mol.66.4 PMID: 15385640

44. Marino S, Hogue IB, Ray CJ and Kirschner DE. A methodology for performing global uncertainty and sensitivity analysis in systems biology. J Theor Biol. 2008; 254:178–196. doi: 10.1016/j.jtbi.2008.04.011 PMID: 18572196

45.   Liu C, Xia X, Wu W, Wu R, Tang M, Chen T, et al. Anti-tumour necrosis factor therapy enhances muco-
       sal healing through down-regulation of interleukin-21 expression and T helper type 17 cell infiltration in
       Crohn's disease. Clin Exp Immunol. 2013; 173(1):102–111. doi: 10.1111/cei.12084 PMID: 23607532